

Electronic Supplementary Information

Prolonging Lifetimes of Plasmonic Hot Electrons for Efficient Hydrogen Evolution by Ag@N,O-C Interfaces with a Unique Ginkgo-leave Hierarchical Structure

Yun Yang,^{†a} Guilin Zhuang,^{†b} Liming Sun,^a Xibo Zhang,^c Wenwen Zhan,^{*a} Xiaojun Wang,^a
Xiguang Han^{*a}

^a*Jiangsu Key Laboratory of Green Synthetic Chemistry for Functional Materials, Department of Chemistry, School of Chemistry and Chemical Engineering, Jiangsu Normal University, Xuzhou, 221116 (P. R. China). E-mail: xghan@jsnu.edu.cn.*

^b*Laboratory of Molecular Catalysis & Computational Materials, Zhejiang University of Technology, Shanghai (P. R. China)*

^c*College of Chemistry and Chemical Engineering, Xiamen University*

[†]*These authors contributed equally*

1. Experiment Section

1.1 Preparation of Ag-precursor:

In a typical synthesis, AgNO₃ (0.017 g, 0.1 mmol) were dissolved in methanol and deionized water mixture solvent (V methanol : V deionized water = 1 : 1). After stirring by ultrasonic concussion for 10 minutes, solution A was obtained. Benzimidazole (0.01 g) is dissolved in a mixed solvent of methanol and water (V methanol : V deionized water = 1 : 1), and after ultrasonication, solution B is obtained. Then, solution B is added to solution A to obtain solution C. Melamine (0.013 g, 0,01 mmol) and PVP (0.05 g) separately dissolved in a mixed solvent of methanol and deionized water (V_{methanol} : V_{deionized water} = 1 : 1), after ultrasonication to obtain solution D; Solution D is added to solution C to obtain solution F. Solution F is reacted in a magnetic stirrer at 90 °C for 4.5 h. After the reaction, the product is collected by centrifugation. It was washed three times with deionized water, then dried at 60 °C overnight.

1.2 Synthesis of Ag@N,O-C Core-Shell Nanoparticles.

Ag@N,O-C were synthesized via calcination of the obtained Ag-precursor at 330 °C for 60 min in Ar atmosphere with heating rate of 5 °C·min⁻¹.

1.3 Characterization

The composition and phase of the as-prepared products were acquired by the powder X-ray diffraction (XRD) pattern using a Panalytical X-pert diffractometer with CuK α radiation. The morphology and crystal structure of as-prepared products were observed by scanning electron microscopy (SEM, SU8100), and high-resolution transmission electron microscopy (HRTEM, FEI Tecnai-F20) with an acceleration voltage of 200 kV. All TEM samples were prepared from depositing a drop of diluted suspensions in ethanol on a carbon film coated copper grid. PHI QUANTUM2000 photoelectron spectrometer (XPS) was using to characterize the surface compositions of product. The surface areas of these samples were measured by the Brunauer-Emmett-Teller (BET) method using nitrogen adsorption and desorption isotherms on a Micrometrics ASAP 2020 system.

1.4 Photoelectric measurement

Photoelectrochemical measurements were performed in a homemade three electrode quartz cell

with a PAR VMP3 Multi Potentiostat apparatus. A Pt plate was used as the counter electrode, and Hg/HgCl₂ electrode was used as the reference electrode. The working electrode was prepared on fluorine-doped tin oxide (FTO) glass that was cleaned by ultrasonication in a mixture of ethanol and acetone for 10 min and dried at 60 °C. Typically, 5 mg of the sample powder was ultrasonicated in 0.2 mL of ethanol to disperse it evenly to get a slurry. The slurry was spread onto FTO glass, whose side part was previously protected using Scotch tape. After air drying, the Scotch tape was unstuck. Then, the working electrode was further dried at 300 °C for 3 h to improve adhesion. The exposed area of the working electrode was 2.5 cm². The cathodic polarization curves were obtained using the linear sweep voltammetry (LSV) technique with a scan rate of 100 mV s⁻¹.

1.5 Photocatalytic activity test

The photocatalytic reaction was carried out in a gas-closed system with a reactor made of quartz. A 300 W xenon lamp was used as a light source. The distance between the lamp and the reactor is 7 cm. In a typical experiment, photocatalyst (5 mg) was added in an aqueous solution (7.2 mL) containing triethanolamine (TEOA, 10 vol%). The mixture was sonicated for 5 min to form a homogeneous suspension. Then, the suspension was irradiated. The amount of hydrogen produced was measured with a gas chromatograph (GC-7900, China, molecular sieve 5A, TCD) using N₂ as a carrier gas.

1.6 Computational details

General Details: All density functional theory (DFT) calculations were performed using the Vienna ab initio simulation package (VASP) [1-3]. Concerning inhomogeneous charge-density distributions, Perdew-Burke-Ernzerhof (PBE) functional with the generalized gradient approximation (GGA) [4] was used to describe the exchange-correlation effect in Kohn-shame equation. Projector-augmented plane wave (PAW) [2] method, featuring the accuracy of all-electron method as well as the efficiency of pseudopotential method, was used to treat inner core and valent electrons. The cutoff energy of 450 eV is used to expand plane wave function basic set. According to Monkhorst-Pack method, the Brillouin zone was sampled under the 3× 3× 2 grid K-points with Γ -pointer center[5], having enough accuracy for energy calculation. The geometrical optimization were carried out by using the conjugated gradient method, and

the convergence thresholds were set to 10^{-5} eV for the energy in and 0.01 eV/Å for Hellmann-Feynman force. A vacuum space larger than 20 Å along the C axis direction was used to avoid interactions of the periodic images.

HER Property: For HER computational parts, two chief mechanisms proposed previously include Volmer-Heyrovsky and Volmer-Tafel mechanisms[7], where the Volmer reaction step ($H^+ + e \rightarrow H^*$) plays an critical role in the whole catalytic reaction. Therefore, Nørskov et. al. proposed that the Gibbs free energy of H^* adsorption (ΔG_{H^*}) is benchmark of evaluating the HER electrocatalytic activity[8]. Assuming the entropy of adsorptive atoms and temperature-dependence of enthalpy is ignored, the Gibbs free energy of absorbed H^* (ΔG_{H^*}) is typically calculated by following formula:

$$\Delta G_{H^*} = \Delta E_{DFT} + \Delta ZPE - T\Delta S$$

Where ΔE_{DFT} , ΔZPE and ΔS are the change of energy from DFT, zero-point energy and entropy of H adsorption, respectively. Both ΔZPE and ΔS are calculated by frequency calculations. Obviously, the negative ΔG_{H^*} means that H is easily adsorbed on the catalyst, but it is difficult to desorb, and vice versa. Therefore, extra overpotential is needed to apply to trigger the generation of H_2 . Generally, the more close to zero the absolute value of ΔG_{H^*} (label as $|\Delta G_{H^*}|$) is, the better activity HER features.

2 Experiment Results

Figure S1 (a) The coordination geometry of central Ag(I) atom in $[\text{Ag}(\text{Bim})]_n$ complex. (b) and (c) The 1D chain structure of $[\text{Ag}(\text{Bim})]_n$ viewed along two different orientations.

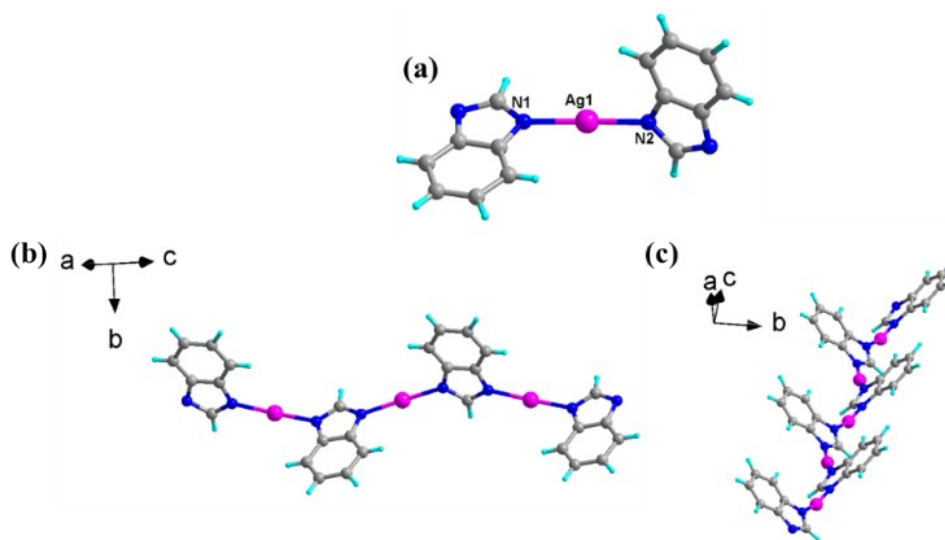


Figure S2 The XRD pattern of $[\text{Ag}(\text{Bim})]_n$ precursor, (b-d) SEM image of $[\text{Ag}(\text{Bim})]_n$ precursor with different magnification. (e-i) The elemental mapping of $[\text{Ag}(\text{Bim})]_n$ precursor.

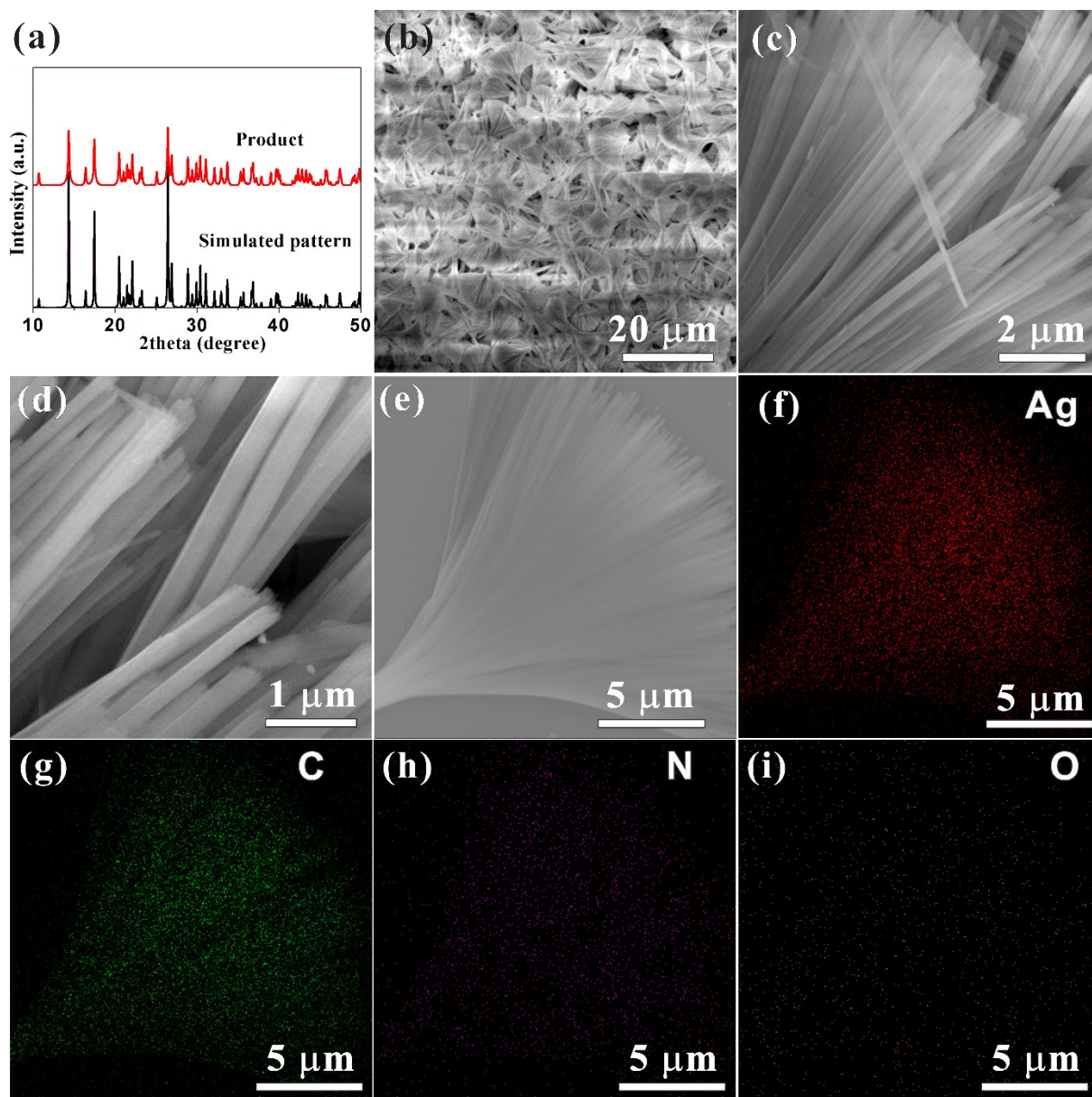


Figure S3 TGA curves of the as-obtained $[\text{Ag}(\text{Bim})]_n$ precursor.

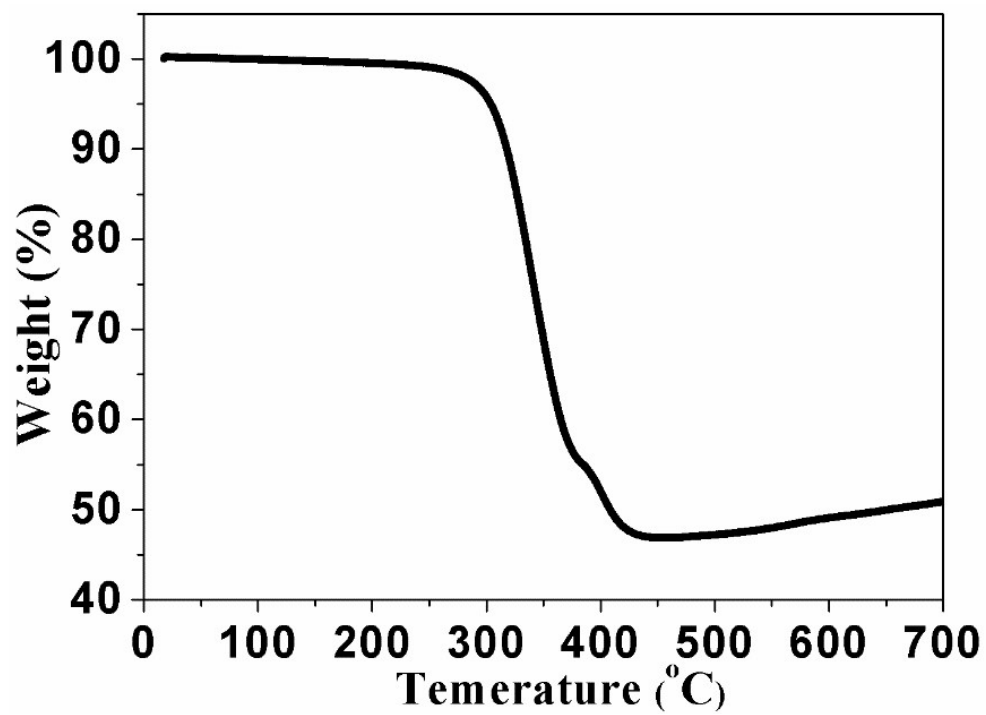


Figure S4 XRD pattern of Ag@N/O-C GLLS.

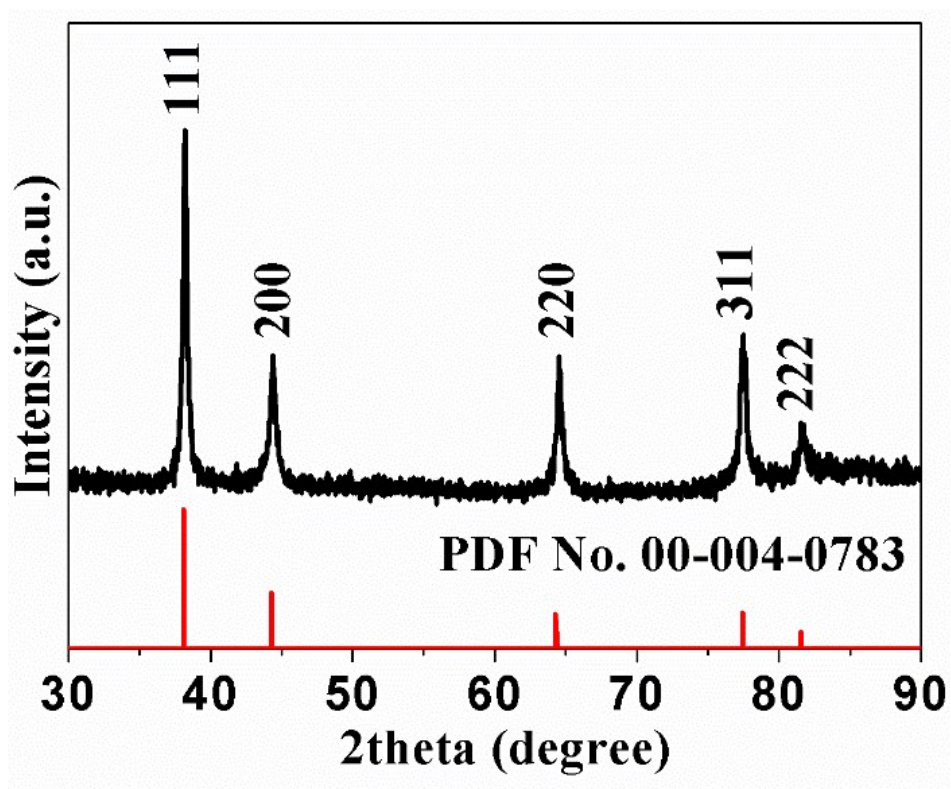


Figure S5 (a) Nitrogen adsorption–desorption isotherms of Ag@N/O-C GLLS, (b) the corresponding pore size distribution.

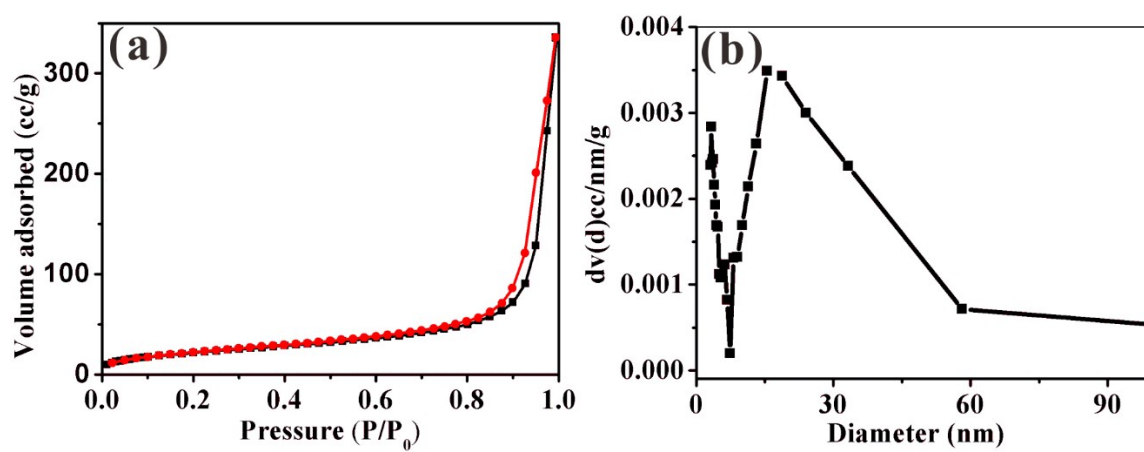


Figure S6 (a) XRD pattern, (b) and (c) SEM image, (d) EDX mapping of N/O-C GLLS.

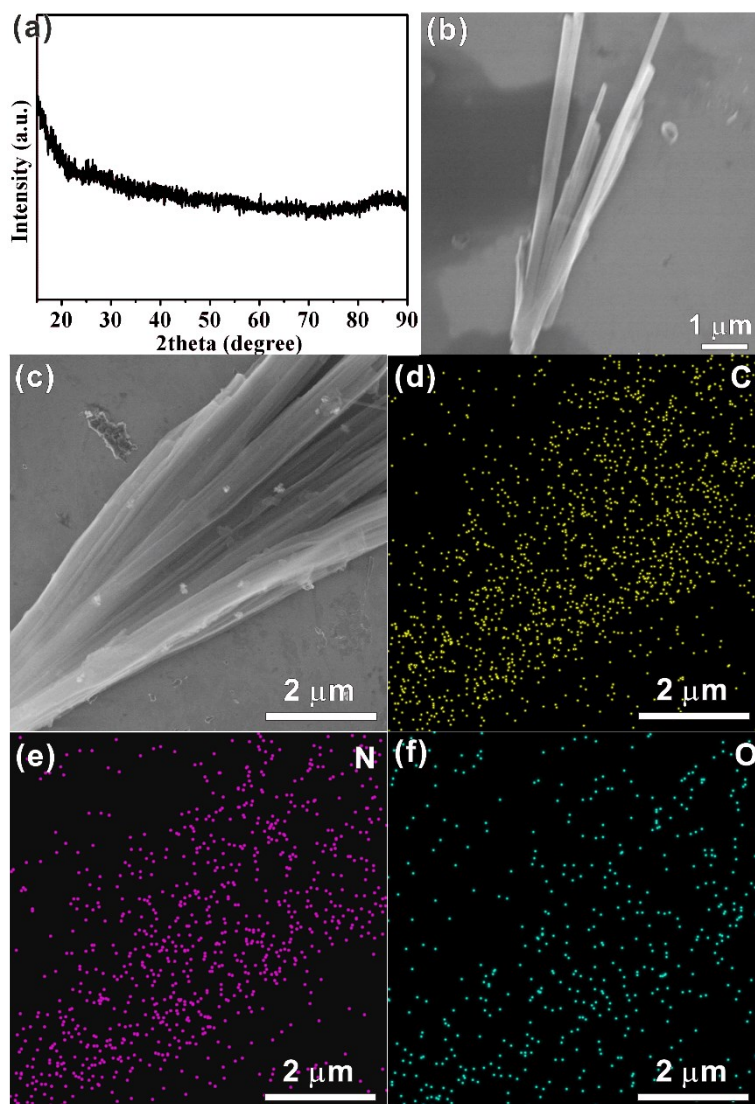


Figure S7 XPS survey spectrum of Ag@N/O-C GLLS.

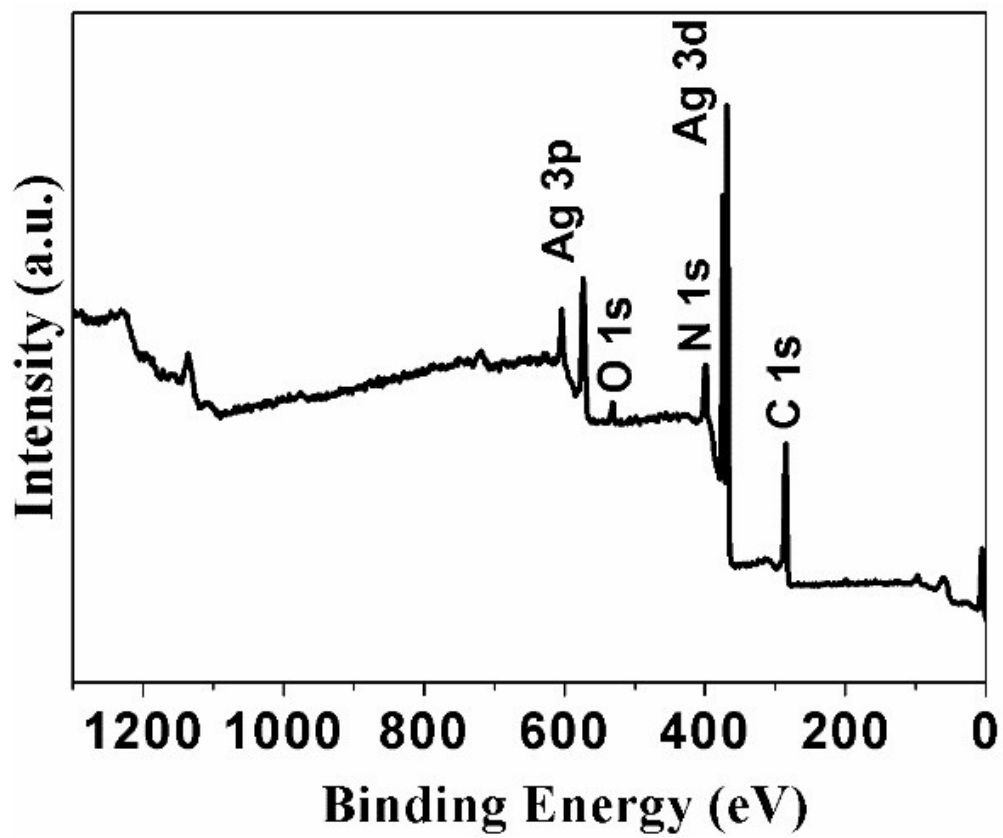


Figure S8 (a) XRD pattern, (b) Raman spectrum, (c) SEM image, (d) EDX mapping of Ag@N/O-C GLLN after O₂ calcination.

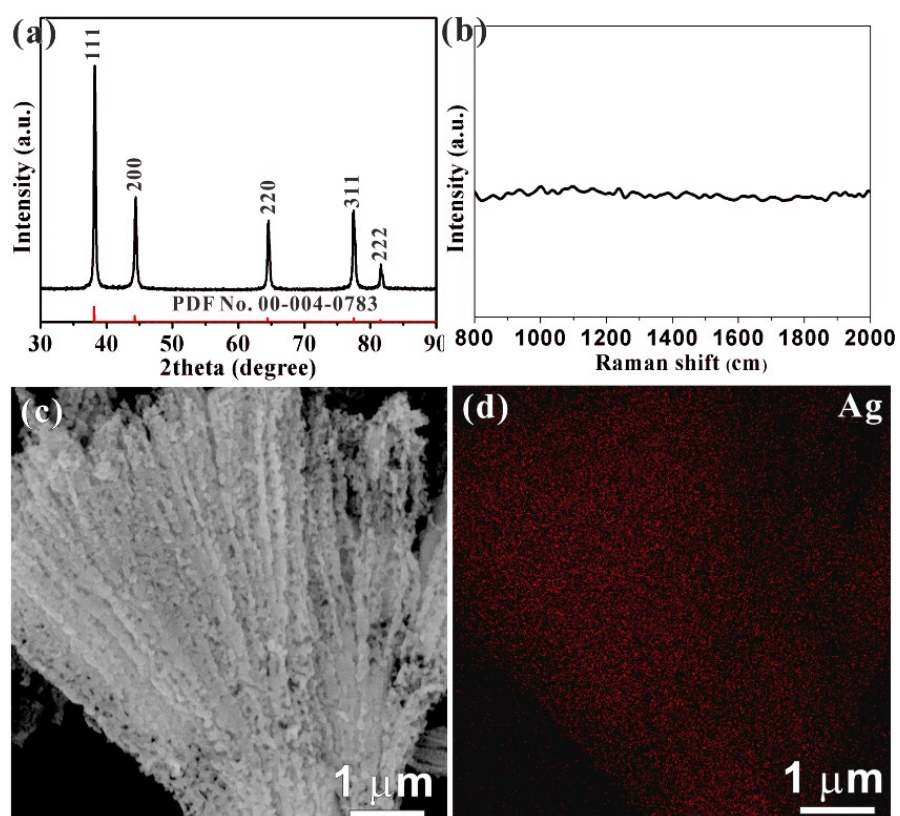


Figure S9 (a) XRD pattern, (b, c) SEM image, (d-f) EDX mapping of Ag+C.

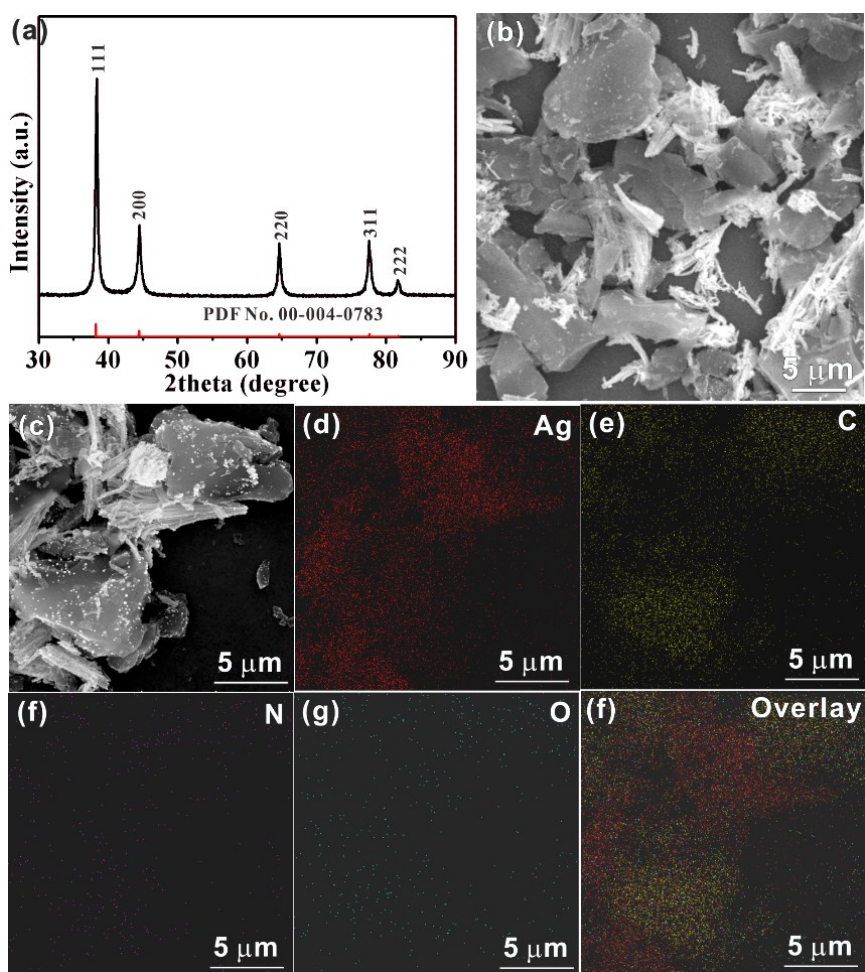


Figure S10 Mass-normalized H₂ yield for 10 h over No catalyst, No TEOA, and Ag@N/O-C.

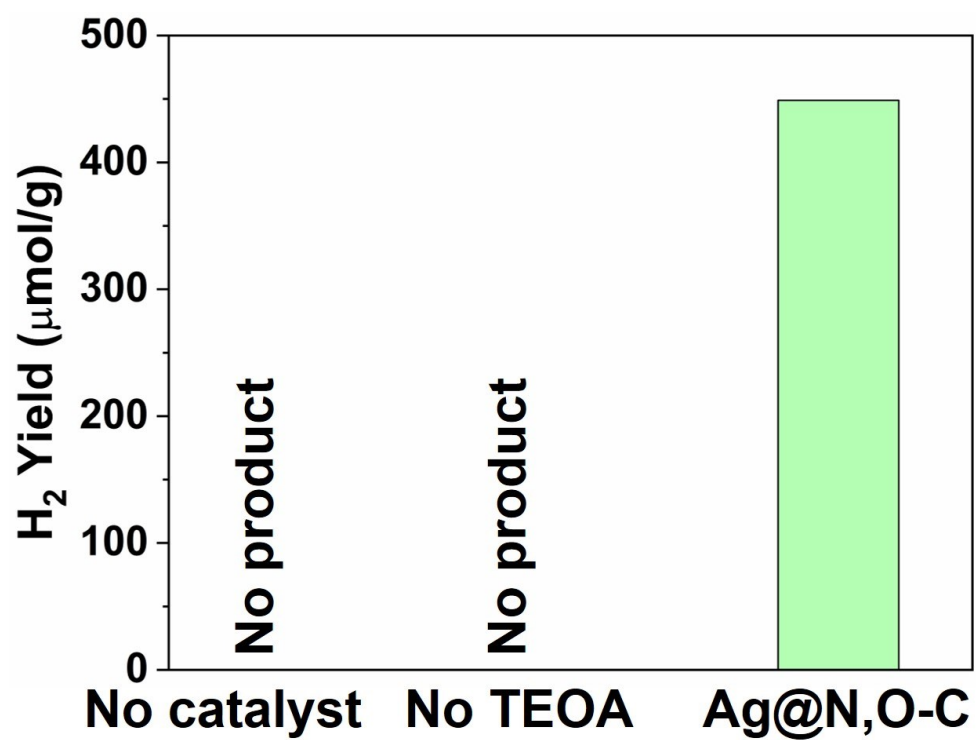


Figure S11. Mass-normalized H₂ yield for 10 h over active carbon and Ag+C.

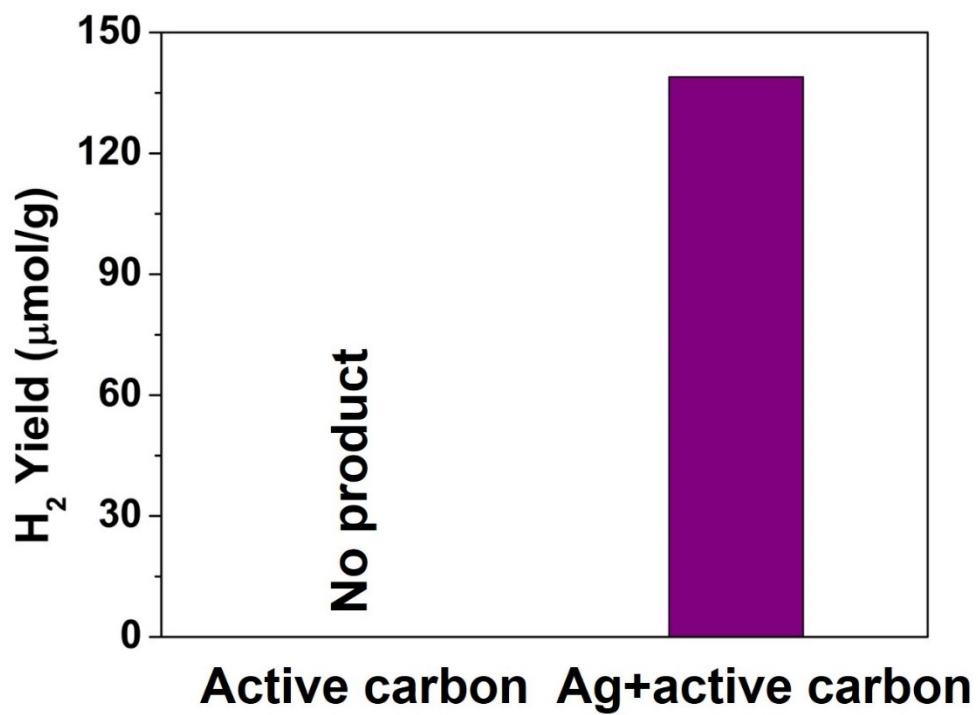


Figure S12 (a) Powder XRD pattern, (b,c) SEM image, and (d-h) EDX elemental mapping of Ag@N/O-C GLLN after catalytic reactions.

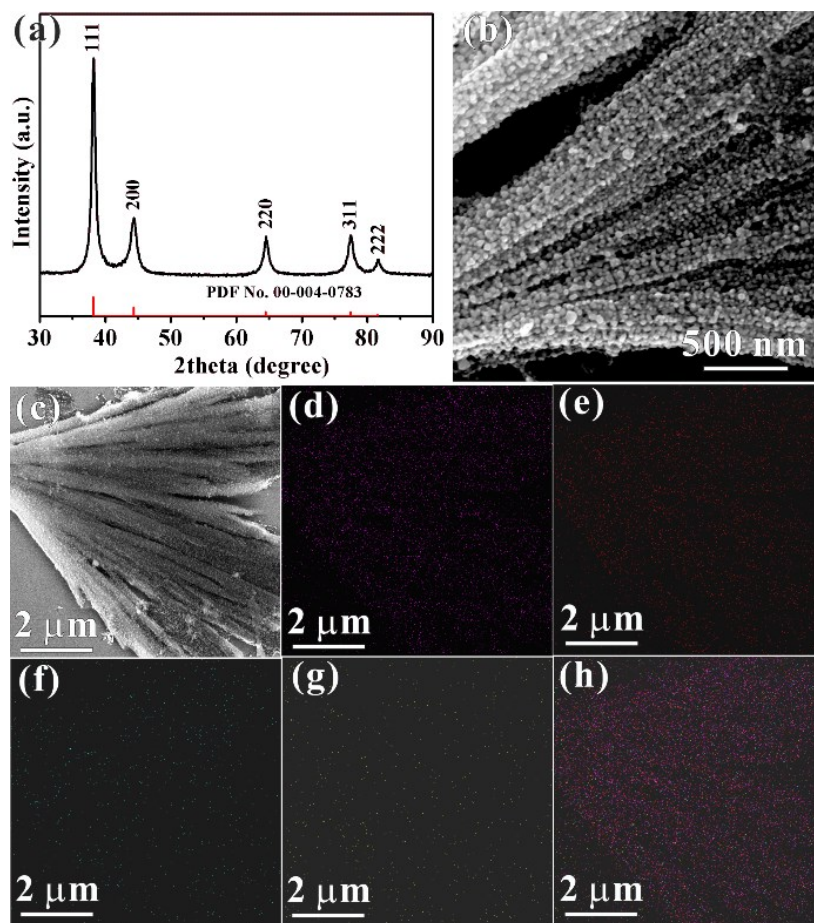
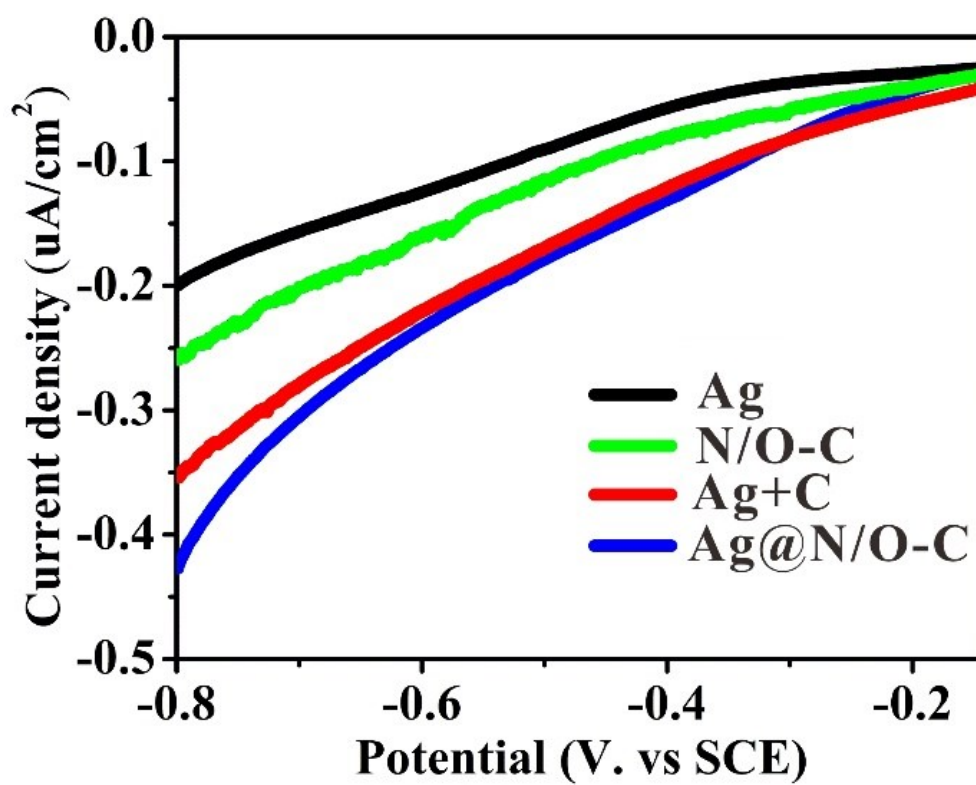


Figure S13 LSV curves of the various samples.



Computational Model:

According to the results from the experimental characterizations (XPS, HRTEM et.al), the as-prepared Ag@N/O-C features monodisperse N, O-doped porous carbon encapsulated Ag nanocrystal with the exposed (111) crystal plane. Under the condition of computational accuracy and huge cost, thus, it can be modeled as N, O-doped porous carbon (consisting of ether oxygen, hydroxyl oxygen) being covered on the surface of 4×4 Ag with exposed crystal plane (111). Subsequently, the initial structure was fully relaxed without any constraint.

Figure S14 Relaxed structure of Ag@N/O-C with top view(a) and side view(b).

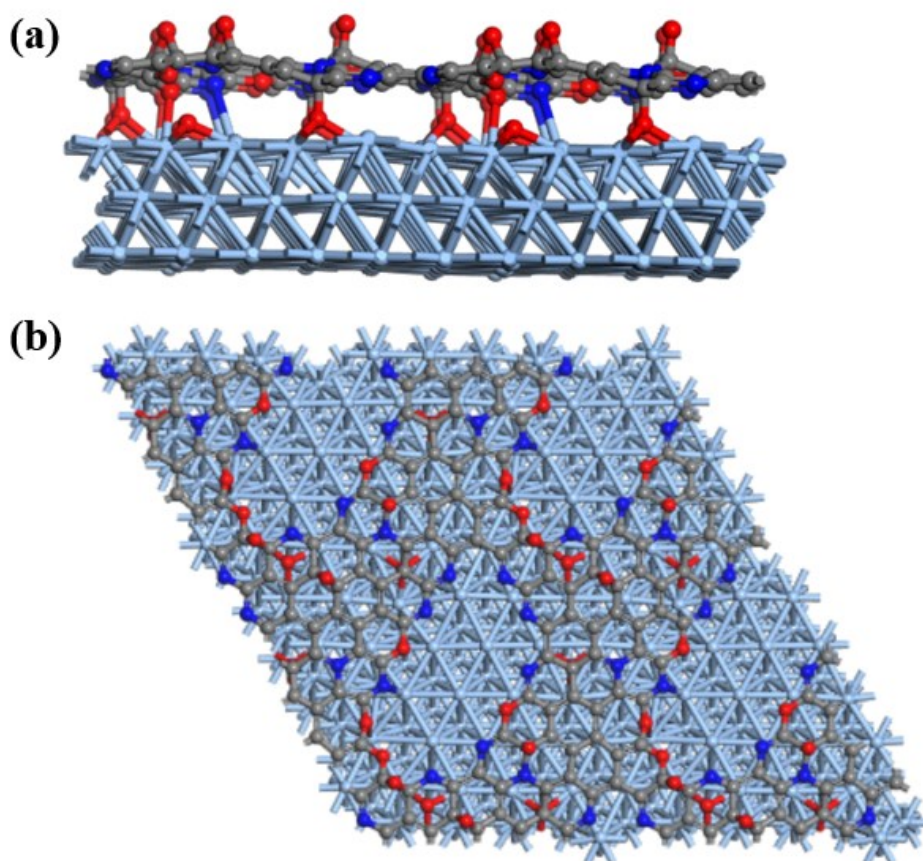
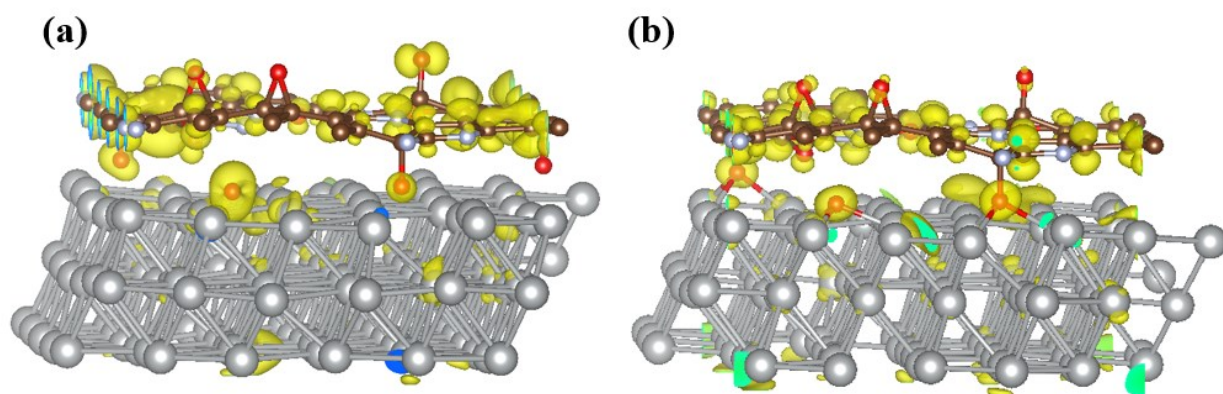


Figure S15 Charge density of Valence band (a) and Conduction band (b).



Reference:

- [1] G. Kresse, J. Hafner, *Phys. Rev. B* **1993**, *47*, 558-561.
- [2] P. E. Blöchl, *Phys. Rev. B* **1994**, *50*, 17953-17979.
- [3] J. P. Perdew, K. Burke, M. Ernzerhof, *Physical Review Letters* **1997**, *78*, 1396-1396.
- [4] Y. Choi, M. Scott, T. Sohnell, H. Idriss, *Phys. Chem. Chem. Phys.*, 2014, *16*, 22588
- [5] S. Grimme , *J. Chem. Phys.* 2006, *27*, 1787.
- [6] H. J. Monkhorst, J. D. Pack, *Phys. Rev. B* **1976**, *13*, 5188-5192.
- [7] N. M. Markovic, P. N. Ross, *Surf. Sci. Rep.* 2002, *45*, 117–229.
- [8] J. K. Nørskov, T. Bligaard, A. Logadottir, J. R. Kitchin, J. G. Chen, S. Pandelov, U. Stimming, *J. Electrochem. Soc.* 2005, *152*, J23.